Measurement of (n,γ) reaction cross section of [186]W-isotope at neutron energy of 20.02±0.58 MeV

Mayur Mehta[a,b*], N L Singh[b], R Makwana[b], P V Subhash[c], S V Suryanarayana[d], S Parashari[b], Rakesh Chauhan[b], R K Singh[b], H Naik[e], S Mukherjee[b], B Soni[b], S Khirwadkar[a], J Varmuza[f] & K Katovsky[f]

[a]Institute for Plasma Research, Gandhinagar 382 428, India

[b]Department of Physics, The M S University of Baroda 390 002, India

[c]ITER-India, Gandhinagar 382 428, India

[d]Nuclear Physics Division, Bhabha Atomic Research Centre, Mumbai 400 085, India

[e]Radiochemistry Division, Bhabha Atomic Research Centre, Mumbai 400 085, India

[f]Department of Electrical Power Engineering, Brno University of Technology, Brno 61600, Czech Republic

The cross-section of [186]W(n,γ)[187]W reaction has been measured at an average neutron energy of 20.02±0.58 MeV by using activation technique. The [27]Al(n,α)[24]Na and [115]In(n,n′)[115m]In reactions have been used for absolute neutron flux measurement. Theoretically the reaction cross-sections have been calculated by using the TALYS-1.9 code. The results from the present work and the EXFOR based literature data have been compared with the evaluated data and calculated data from TALYS-1.9 code.

1 Introduction

Tungsten is considered to be a prime plasma facing material used as divertor component in ITER like fusion reactor. For the design and safety of nuclear reactors, accurate data of reaction cross-section needed for materials used in reactors[1-4]. There are large discrepancies and deficiencies of the neutron induced reaction cross-section data in a range from 5 to 20 MeV. This work provides the detail measurement of [186]W(n,γ)[187]W reaction cross-section at an average neutron energy (E_n) of 20.02±0.58 MeV using activation and off-line γ-ray spectrometric technique. Theoretically the reaction cross-section was predicted by the nuclear modular codes TALYS-1.9[5]. The experimentally measured cross-section was compared with Experimental Nuclear Reaction Data (EXFOR)[6] and Evaluated Nuclear Data File (ENDF)[7].

2 Experimental Details

The experimental work was carried out at 6 meter height of beam line of Pelletron facility at Tata Institute of Fundamental Research-Bhabha Atomic Research Center (TIFR-BARC)-Mumbai. The neutrons of desired energy was generated by the [7]Li(p,n)[7]Be reaction[8,9] using 14UD BARC-TIFR Pelletron facilities at Mumbai, India. The proton beam energy of 22 MeV was passed through Tantalum–Lithium–Tantalum (Ta-Li-Ta) stack to generate neutron energy of 20.02±0.58 MeV. During the experiment, the beam current was about 150-170 nAmps. A natural Li metal foil of thickness 6.8 mg/cm² was wrapped between Ta foils of thickness 3.2 mg/cm² in front and 0.025 mm in the back side. According to SRIM [10] calculation, the degradation of proton energy was ~50 keV.

Plansee natural tungsten (W) metal sample of thickness 3 mm and size 10×10 mm was used for irradiation. Aluminum (Al) and indium (In) foils of thickness 0.1 mm and 10×10 mm size were used as flux monitor via [27]Al(n,α)[24]Na and [115]In(n,n′)[115m]In reactions. Tungsten and monitor samples (Al and In) were wrapped with 0.025 mm thick aluminum foil to avoid contamination during the irradiation. In-W-Al stack was placed at 0º in forward direction to the beam at a distance of distance of 2.1 cm. To determine accurate value and minimize the error in neutron flux incident on the target sample Al and In

*Corresponding author (E-mail: mayur@ipr.res.in)

foils were used as flux monitors. The nuclear spectroscopic data of reaction products are given in Table 1 retrieved from Ref.[11]. A schematic diagram of experimental set up was shown in Fig. 1.

The stack was irradiated for 5-6 h and then cooled for sufficient hours. Then the irradiated samples were mounted on Perspex plates for γ-ray activity measurement. Pre-calibrated 80 cm³ High Purity Germanium (HPGe) detector was used for the γ-ray counting of the irradiated samples. To avoid the summation effect, the mounted samples were placed at a suitable distance from the detector cap. The resolution of the detector system had a full-width at half-maximum of 1.8 keV at 1.332 MeV γ-ray photo-peakof [60]Co. The energy and efficiency calibration was performed by using standard [152]Eu multi-gamma source, maintaining the same geometry[12].

3 Data Analysis

3.1 Measurement of average neutron energy and neutron flux

The spectrum averaged neutron energy was calculated by using the following equation[13]:

$$E_{mean} = \frac{\int_{E_{ps}}^{E_{max}} E_i \Phi_i dE}{\int_{E_{ps}}^{E_{max}} \Phi_i dE} \qquad \ldots(1)$$

where, E_{mean} is effective mean energy ,E_{ps} is starting of neutron energy peak, E_{max} is maximum neutron energy, E_i is energy bin and Φ_i is neutron flux of energy bin E_i.

Figure 2 represents the continuous neutron spectrum for Eproton= 22 MeV. A detailed discussion on the generation of neutron spectra is also provided in our earlier publications[14-17]. The reported cross-sections from the neutron spectrum were found in agreement with the literature and theoretical data for the respective case of study. One of the collaborators Katovsky (Department of Electrical Power Engineering, Brno University of Technology, Brno, Czech Republic) performed MCNP6.1 calculations for the neutron spectrum generation using the defined geometry of the target assembly for 22 MeV energy protons. The simulated spectra were found in agreement with the theoretical reproductions from the previous works[18-20]. Minor discrepancies, however, may be found among the compared results. A rough estimation of the neutron flux using the simulated spectra were found in agreement with the flux used in the present work within the uncertainty of ≈3%. The uncertainty due to the neutron flux was already used in the weighted cross-sections of monitor reaction from EXFOR library. At this point, we cannot re-calculate the entire calculations as the results from the simulate spectra lies within the range of present
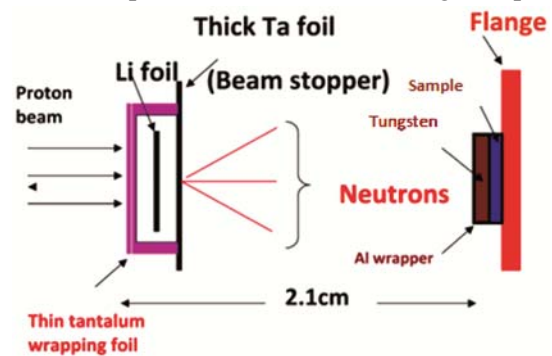

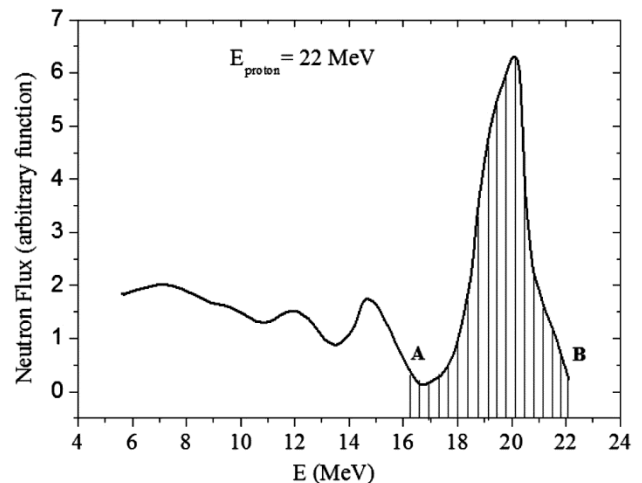Fig. 1 — Schematic diagram of irradiation set up.

Fig. 2 — Neutron spectrum for E_{proton}= 22 MeV with low energy tail.

Table 1— Nuclear spectroscopic data of reaction products from Ref.[19].

Reaction	Threshold energy (MeV)	Half-life	Decay mode	γ-ray energy (keV)	γ-ray abundance (%)
[115]In(n,n′)[115m]In	--	4.486h	IT (95%) β⁻ (5%)	336.24	45.83
[27]Al(n,α)[24]Na	3.249	14.959h	β⁻ (100%)	1368.63	100
[186]W(n,γ)[187]W	--	23.72h	β⁻ (100%)	479.531 685.774	21.8 27.3

results. The recorded neutron spectrum on target sample has a long tail in the lower energy region. In order to measure the reaction cross-section at the main peak of neutron energy, the tailing correction has been done by using the method given in literature[17]. Figure
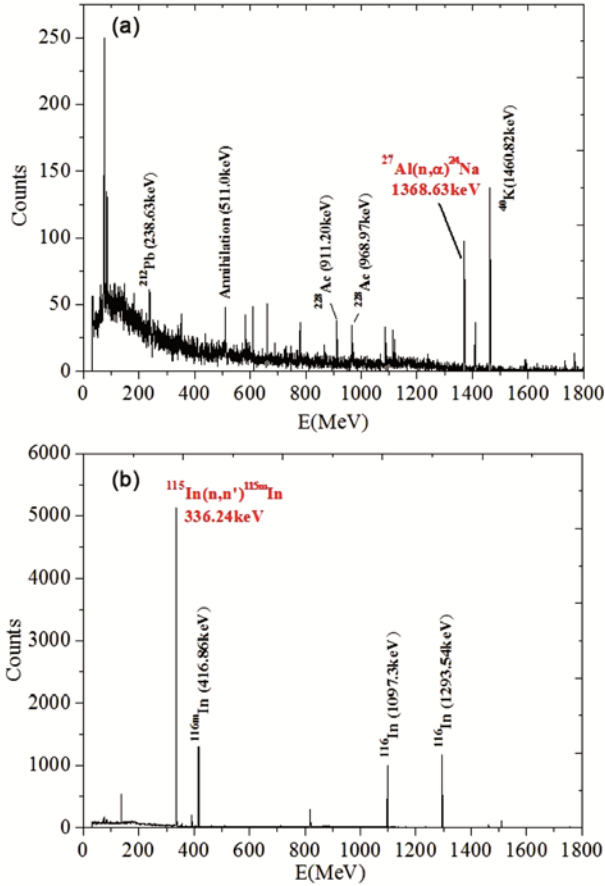

Fig. 3 — (a) Recorded γ-ray spectra of products from the monitor reactions and (b) recorded γ-ray spectra of products from the monitor reactions.
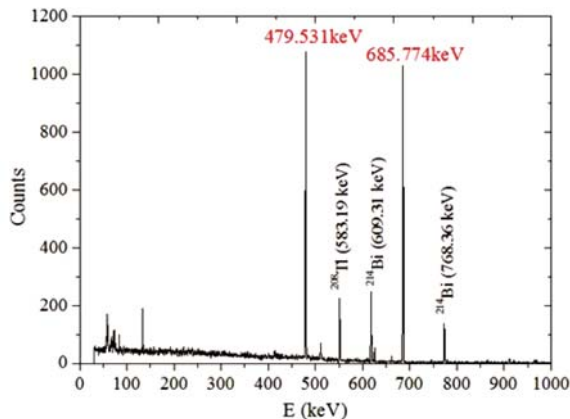

Fig. 4 — Recorded γ-ray spectrum of reaction products from the [186]W(n,γ)[187]W reaction.

3(a,b) and Figure 4 show γ-ray spectra of monitor reaction and sample reaction products.

The neutron flux was determined by $^{27}Al(n,\alpha)^{24}Na$ ($t_{1/2}$=14.959 hour, E_γ=1368.63 keV) and $^{115}In(n,n')^{115m}In$($t_{1/2}$=4.486 hour, E_γ=336.24 keV) monitor reactions. In order to calculate the neutron flux incident on the sample, the spectrum averaged cross-section was calculated for the monitor reaction by using the available data from EXFOR [6]. The spectrum averaged cross-section was calculated by using equation:

$$\sigma_{av} = \frac{\int_{E_{th}}^{E_{max}} \sigma_i \Phi_i dE}{\int_{E_{th}}^{E_{max}} \Phi_i dE} \qquad \dots (2)$$

where, σ_{av} is spectrum averaged cross-section, E_{th} is threshold energy of the monitor reaction, E_{max} is maximum neutron energy, σ_i is cross-section of monitor reaction at energy E_i from EXFOR data, Φ_i is neutron flux of energy bin E_i.

The γ-ray spectrum of monitors is shown in Fig. 3. The spectrum averaged cross-section and the neutron flux measured by using the activation formula is given in Table 2.

$$\Phi = \frac{A_\gamma \lambda \left(CL/LT\right)}{N\sigma_{av}I_\gamma\varepsilon(1-e^{-\lambda t_i})(1-e^{-\lambda t_c})e^{-\lambda CL}} \qquad \dots (3)$$

where, A_γ is number of photo peak counts, λ is decay constant of reaction (sec^{-1}), N is number of target atoms, σ_{av} is spectrum averaged cross-section, I_γ is absolute γ-ray intensity, ε is efficiency of the γ-ray of interest, t_i is time of sample irradiation(sec), t_c is cooling time (between the end of irradiation and start of counting in sec), CL is clock time and LT is live time for counting and CL/LT term is used for dead time correction.

3.2 Measurement of $^{186}W(n,\gamma)^{187}W$ reaction cross-section

The cross-section of $^{186}W(n,\gamma)^{187}W$ reaction was measured by using photo peak activity of 479.531 and 685.774keV γ-ray of ^{187}W isotope. The equation used to measure the reaction cross-section is as follows:

$$\sigma = \frac{A_\gamma \lambda \left(\frac{CL}{LT}\right)}{N\Phi I_\gamma\varepsilon(1-e^{-\lambda t_i})(1-e^{-\lambda t_c})e^{-\lambda CL}} \qquad \dots (4)$$

All terms in Eq. (4) have a significance meaning as in Eq. (3).

Table 2 — Spectrum average cross-section and measured neutron flux from monitor reactions.

E_n (MeV)	Spectrum Average Cross-section (mb)		Neutron Flux (ncm^{-2}s^{-1})	
20.02±0.58	^{115}In(n,n′)^{115m}In	^{27}Al(n,α)^{24}Na	^{115}In(n,n′)^{115m}In	^{27}Al(n,α)^{24}Na
	150.43	60.59	3.39x10^6	3.36x10^6

Table 3 — Comparison of measured reaction cross-section with the evaluated data and calculated data from TALYS-1.9.

E_n (MeV)	^{186}W(n,γ)^{187}W reaction cross-section (in mb)				
20.02±0.58	Measured	TALYS-1.9	ENDF/B-VIII.0	JEFF-3.3	JENDL-4.0
	0.3656± 0.031	0.4472	0.35834	0.4881	0.2526

4 Results and Discussion

As shown in Fig. 2, the neutron spectra have tail part in lower energy range. This low energy neutron tail part will cause contribute to the measured reaction cross-section. The experimentally measured cross-section of ^{186}W(n,γ)^{187}W at neutron energy of 20.02±0.58 MeV is 0.5531 mb and the contribution due to low energy neutron tail part of spectrum is 0.1875 mb as calculated based on Ref. [21]. Thus for an average neutron energy of 20.02±0.58 MeV, after subtracting the contribution from the low energy neutron tail region, the actual experimentally obtained ^{186}W(n,γ)^{187}W cross-sections was found to be 0.3656 mb. Table 3 shows the comparison of experimentally measured reaction cross-section with theoretically predicated data by TALYS-1.9 and available literature data. Theoretically the reaction cross-section as a function of neutron energy (E_n) was calculated by TALYS-1.9 code using default parameters as well as by different parameters such as γ-strength functions, nuclear level densities and nuclear model parameters etc. In present case we predict the reaction cross-section by considering different level density parameters such as constant temperature + Fermi gas model, Back-shifted Fermi gas model, Generalised super fluid model and Microscopic level densities options available as LD model-1 to LD model-6. Figure 5 shows the comparison of ^{186}W(n,γ)^{187}W reaction cross-section with the previously measured data by different authors[17,22-25] as well as literature data available in nuclear data library[7] and the predicated values based on TALYS-1.9 code [5]. From Table 3 and Fig. 5, it is observed that the cross-section of ^{186}W(n,γ)^{187}W reaction is in excellent agreement with the evaluated data from ENDF/B-VIII.0 library and is in close agreement with TALYS-1.9 and JEFF-3.3 at the neutron energy of 20.02±0.58 MeV. It can also be seen from Fig. 5 that, present and literature data within the neutron energies of 2-24 MeV follow a close trend of the calculated values from TALYS-1.9
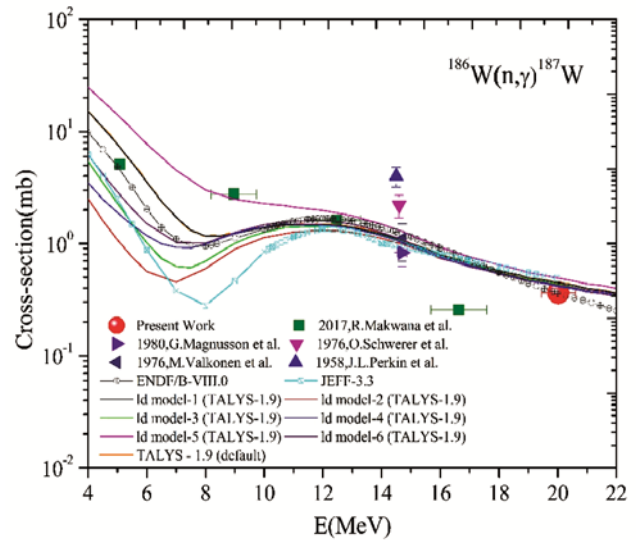

Fig. 5 — Comparison of ^{186}W(n,γ)^{187}W reaction cross-section with literature data, evaluated data from different libraries and calculated values from TALYS-1.9 code.

code and evaluated data of ENDF/B-VIII.0 library but not of JEFF-3.3 library at lower neutron energy.

5 Conclusions

In present work, the cross-section of ^{186}W(n,γ)^{187}W reaction was measured first time experimentally at the neutron energy of 20.02±0.58 MeV by using neutron activation method. The measured reaction cross-section of tungsten isotope was compared with the theoretically predicated data from TALYS-1.9 and data available in evaluated cross-section data libraries, which show a close agreement.

References

1   Pintsuk G, *Comp Nucl Mater*, 4 (2012) 551.
2   Nygren R E , Youchison D L , Wirth B D & Snead L L, *Fusion Eng Design*,109 (2016) 192.
3   Forrest R A, *Fusion Eng Design*, 81 (2006) 2143.
4   Wenrong Z, Hanlin L, Weixiang Y & Xialin Y, Compilation of measurement and evaluations of nuclear activation cross section for nuclear data applications, INDC (CPR)-16 (1989).
5   Koning A J, TALYS-1.9, A Nuclear reaction program, user's manual, NRG-1755 ZG Petten, The Netherlands (2018).
6   EXFOR, Cross Section Information Storage and Retrieval System (EXFOR), IAEA, Vienna, Austria, ⟨http://www.nds.iaea.or.at/exfor/(online)⟩
7   ENDF, Cross Section Information Storage and Retrieval System (EXFOR), IAEA, Vienna, Austria, <https://www-nds.iaea.org/exfor/endf.htm(online)>
8   Poppe C H & Anderson J D, *Phys Rev C*, 14 (1976) 438.
9   Mashnik S G, Chadwick M B, H Hughes G, Little R C, Macfarlane R E, Waters L S & Young P G, ^{7}Li(p, n) Nuclear data Library for Incident Proton Energies to 150MeV, arXiv: nuclth/00110666v117.
10 Ziegler J F, *Nucl Instr Meth Phys Res B*, 219-220 (2004) 1027.
11 National Nuclear Data Center, http://www.nndc .bnl. gov/nu dat2/index.jsp
12 Yerraguntla S S, Naik H, Karantha M, Ganesan S, Saraswatula S V & Nair S N P, *Radiochim Acta*, 106 (2018) 877.
13 Smith D L, et al., Corrections for Low Energy Neutrons by Spectral Indexing, retrieved from https://www.oecdnea.org/ science/docs/2005/nsc-wpec-doc2005-357.pdf.
14 Bhargav S, Siddharth P, Mukherjee S, Makwana R, Suryanarayana S V, Nayak B K, Naik H, Varmuza J & Katovsky K, *Eur Phys J Plus*, 300 (2020) 135.
15 Parashari S, Mukherjee S, Suryanarayana S V, Nayak B K, Makwana R, Singh N L & Naik H, *Phys Rev C*, 99 (2019) 044602.
16 Parashari S, Mukherjee S, Naik H, Suryanarayana S V, Makwana R, Nayak B K & Singh N L, *Eur Phys J A*, 51 (2019) 55.
17 Makwana R, Mukherjee S, Mishra P, Naik H, Singh N L, Mehta M, Katovsky K, Suryanarayana S V, Vansola V, Sheela Y S, Karkera M, Acharya R & Khirwadkar S, *Phys Rev C*, 96 (2017) 024608.
18 Liskien J H & Paulsen A, *Atomic Data Nucl Data Table*, 15 (1975) 57.
19 Meadows J W & Smith D L, Neutrons from Proton Bombardment of Natural Lithium, Argonne National Laboratory Report ANL-7983 (1972).
20 McNaughton M W, King N S P, Brady F P, Romero J L & Subramanian T S, *Nucl Instr Meth*, 130 (1975) 555.
21 Badwar S, Ghosh R, Lawriniang B M , Vansola V, Sheela Y S, Naik H, Naik Y, Suryanarayana S V, Jyrwa B & Ganesan S, *Appl Radiat Isot*, 129 (2017) 117.
22 Perkin J L, Oconnor L P & Coleman R F, *Proc Phys Soc*, 72 (1958) 505.
23 Magnusson G, Andersson P & Berquist I, *Physica Scripta*, 21 (1980) 21.
24 Valkonen M, Homberg P, Rieppo R, Keinaenen J K & Kantele J, *Phys Lett B*, 39 (1976) 625.
25 Schwerer O, Winkler-Rohatsch M, Warhanek H & Winkler G, *Nucl Phys A*, 264 (1976) 105.